DEUTSCHES ELEKTRONEN-SYNCHROTRON DESY

DESY SR-80/14
October 1980

A SCANNING ULTRASOFT X-RAY MICROSCOPE WITH MULTILAYER COATED REFLECTION OPTICS: FIRST TEST WITH SYNCHROTRON RADIATION AROUND 60 eV PHOTON ENERGY

by

R.-P. Haelbich

II. Institut für Experimentalphysik der Universität Hamburg
and
Hamburger Synchrotronstrahlungslabor HASYLAB
at
Deutsches Elektronen-Synchrotron DESY, Hamburg

NOTKESTRASSE 85 · 2 HAMBURG 52

DESY SR-80/14
October 1980

A SCANNING ULTRASOFT X-RAY MICROSCOPE WITH MULTILAYER COATED REFLECTION OPTICS: FIRST TEST WITH SYNCHROTRON RADIATION AROUND 60 eV PHOTON ENERGY

R.-P. Haelbich

II. Institut für Experimentalphysik
Universität Hamburg, D 2000 Hamburg 50
and
Hamburger Synchrotronstrahlungslabor HASYLAB
Deutsches Elektronen-Synchrotron DESY
D 2000 Hamburg 52, Federal Republic of Germany

1. INTRODUCTION

Ultrasoft X-rays (10 Å < λ < 100 Å) are of special interest in the microscopy of biological samples. The composition can be identified without staining, the value of the absorption index allows good contrast for the typical thickness of cell components, and the resolution can be improved compared to that of the light microscope due to the shorter wavelength. In contrast to electron microscopy, examination of live samples in wet environment can be easily accomplished between transparent membranes, radiation damage is smaller, and examination of thicker samples is possible.

When synchrotron radiation became available as the brightest source of ultrasoft X-rays having a continuous spectrum, microscopy in this spectral range regained interest. Contact microscopy (Gudat, 1978) works very successfully without optical elements. Schmahl, Rudolph, Niemann and Christ (1980) use Fresnel zone plates as lenses in an instrument which produces real magnified pictures. For another new field, the diagnostics of laser fusion plasmas microscopes with mirror optics at grazing incidence have been built (Silk, 1980). Although mirror optics for normal incidence would be advantageous, since aberrations are much smaller than for grazing incidence, and larger apertures can be realized, they have not been considered so far, since the reflectivities of mirror coating materials are smaller than a tenth of a percent at wavelengths below 100 Å.

Stimulated by calculations of Spiller (1972) we were able to demonstrate that also the reflectivity in the vacuum ultraviolet and soft X-ray region can be enhanced by multi-

to be published in: Proceedings of the conference on "Scanned Image Microscopy", London, Sept. 22-24, 1980.

layer coatings (Haelbich and Kunz, 1976; Haelbich, Segmüller and Spiller, 1979). Based on these results we have built the prototype of a microscope with mirror optics for normal incidence operating at $\lambda = 200$ Å. A combination of two spherical mirrors as suggested by Schwarzschild (1905) is sufficient for a correction of aberrations. The important advantage is that spherical mirrors can be produced with a better optical figure and smaller surface roughness than aspherical ones. Therefore, we did not consider an elliptical mirror. By means of the Schwarzschild type objective a highly demagnified image of the source is produced and the sample is mechanically scanned along this light probe while the transmitted light is recorded. This scanning version is given preference to a conventional setup, because the radiation dose for the sample is smaller, the imaging properties of the objective are better and the microscope is easier to handle.

In addition to the results with the prototype I shall discuss the future prospects of our method and present ray tracing calculations which reveal the excellent imaging properties of the spherical mirror pair.

2. EXPERIMENT

Setup of the Microscope

The construction of the prototype of a microscope with reflection optics for normal incidence should serve as a test of the principal problems. Since the resolution can be tested also with one-dimensional line scans, we did not install an expensive system for recording and displaying two-dimensional images.

The experimental setup is illustrated in Fig. 1. The electron beam of the DESY synchrotron forms a light source of 2 mm vertical and 10 mm horizontal extension. Demagnification is carried out in two steps. For the first step a mirror at grazing incidence can be used, because the imaging errors involved there are still tolerable. A focussing paraboloid which is part of an existing monochromator serves this purpose (while the grating of the monochromator is used in zeroth order as another mirror). The factor of demagnification is 40:1 and a pinhole at the site of the focus of the paraboloid reduces the intermediate image further to a circle of 50 μm in diameter. In a second step, a multilayer coated Schwarzschild type objective 1 m behind the pinhole projects a 74 times reduced image onto the specimen.

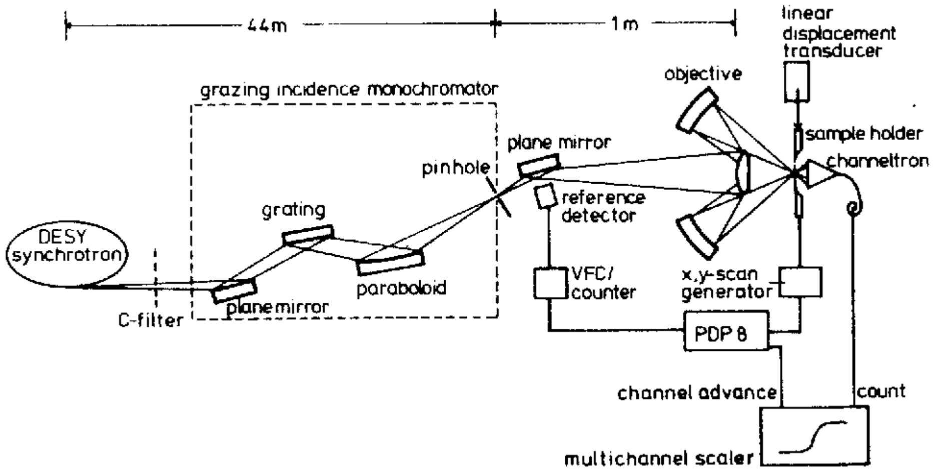

Fig. 1. Prototype of the scanning ultrasoft X-ray microscope. The first step of demagnification is done by a paraboloid for grazing incidence, the second step by a Schwarzschild type objective. The grating of the monochromator is used in the direct image.

The sample is mounted on optical slides and can be aligned by micrometer screws in three directions. It is scanned by piezoelectric transducers which are controlled with the help of a minicomputer (PDP 8e) and agitated by a programmable high voltage supply. The smallest stepsize is 100 Å, the maximum range 40 μm. Since the piezoelectric transducers exhibit a strong nonlinearity and some drift (Staehr, 1980), the position cannot be monitored by the applied voltage, but by inductive transducers with a resolution better than 500 Å.

The photons transmitted by the specimen are detected by a channeltron and counted by a multichannel scaler whose channels are related to the position on the sample. Since the photonflux of the synchrotron varies considerably, we use a reference detector which measures the photoelectric yield of a gold coated mirror. This signal is digitized by a voltage to frequency converter and counted. At a preset value the computer advances the multichannel scaler and the scanning stage.

Some aspects of the experimental setup will be discussed in detail below.

Multilayer Interference Coatings

The normal incidence reflectivity of metals decreases strongly above the plasma energy. For heavy metals this limit lies at approximately 40 eV. At a photon energy of 60 eV, the reflectivity of the best mirror materials is in the order of one percent (Hagemann, Gudat and Kunz, 1975) and decreases further roughly proportional to λ^4. At oblique incidence the wavelength limit shifts to smaller wavelengths; therefore, mirror optics are used at grazing incidence in the photon energy region $h\nu > 40$ eV.

In X-ray physics, crystals are good reflectors at any angle of incidence, when all their lattice planes add in phase to the reflected wave. Higher flexibility in the choice of lattice constants can be achieved by evaporating alternating layers of highly and weakly absorbing materials (Spiller, 1972). As with natural crystals, the superposition of the incident and the reflected beam produces a standing wavefield with the nodes in the highly absorbing layers; therefore, the penetration depth is considerably enlarged and a great number of layers contribute to the reflected beam.

Suitable materials for a multilayer coating should not only have a large difference in the optical constants , but should also form stable and smooth boundaries and be chemically inert. The thickness of a single layer is in the order of $\lambda_{max}/4$, where λ_{max} is the wavelength of maximum reflectivity. The best results have been obtained with ReW alloy (Haelbich *et al.*, 1979) and AuPd alloy (Spiller, Segmüller, Rife and Haelbich, 1980b) as highly absorbing materials and C or B as weakly absorbing material.

The left side of Fig. 2 shows one of our best results of the near-normal-incidence reflectivity of a multilayer coating with three, five and seven layers of ReW and C in comparison to a single thick film of ReW (Haelbich *et al.*, 1979). The three and five layer coatings were obtained by shadowing part of the wafer with a shutter during evaporation. The peak reflectivity increases with the number of periods, but the width of the peaks decreases and, therefore, the integral under the reflectivity curve grows more slowly than the peak reflectivity. Thus, the reflector also acts as a coarse monochromator, its bandwidth depending on the number of periods. In order to obtain a good contrast in soft X-ray microscopy, coarse monochromaticity is needed and the multilayer coatings on the objective mirrors make extra monochromatisation unnecessary.

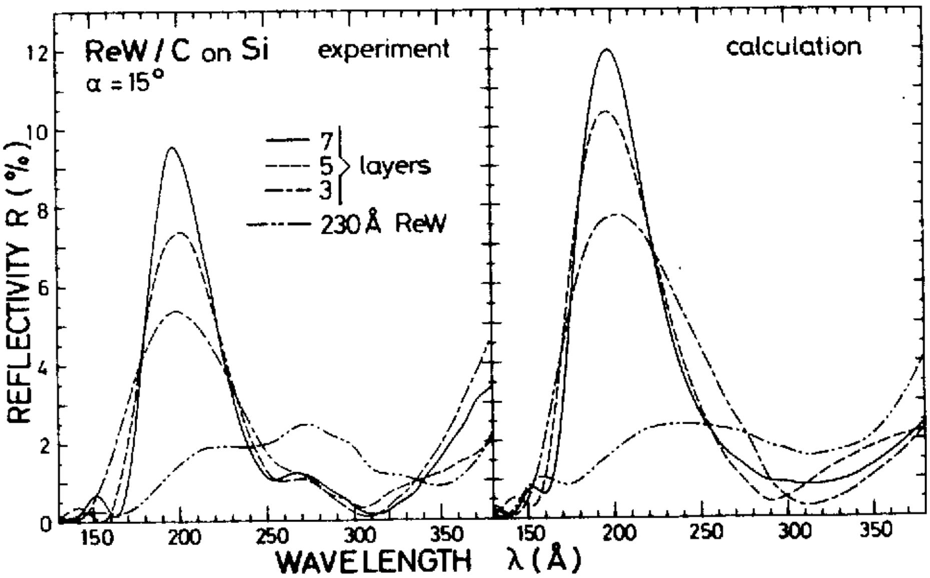

Fig. 2. Experimental (left) and calculated (right) reflectivity of a 230 Å thick film of ReW and of a three, five and seven-layer coating of ReW and C at an angle of incidence of α = 15°. The optical constants used for the calculations are taken from Haelbich (1980) for ReW and the Si substrate and Hagemann et al. (1975) for C. The thickness of the layers starting at the Si substrate with ReW are: 57.8, 60.9, 50.7, 63.8, 48.0, 65.6, 50.2 Å.

The theoretical curves shown on the left side of Fig. 2 are calculated with optical constants from Hagemann *et al.* (1975) for C and Haelbich (1980) for ReW and the Si substrate. The comparison with the experimental curves demonstrates that the multilayers show almost the theoretically attainable performance.

The most critical point in producing these multilayers is the exact control of the film thickness. Monitoring the film thickness with an oscillating quartz crystal leads in general to statistical errors with the result that not all layers contribute in phase to the reflected beam. For shorter wavelengths, where more and thinner layers are necessary to obtain high reflectivity, a new method of thickness control has been developed by Spiller, Segmüller and Haelbich (1980a).

The smoothness of the films is also important for good near-normal-incidence reflectivity. Haelbich *et al.* (1979)

have shown that diffuse scattering from multilayers with up to 11 layers is the same as from a single thick film with a root mean square surface roughness of $\sigma = 3$ Å. This means that scattering is negligible at $\sigma = 200$ Å.

The Schwarzschild Type Objective

Schwarzschild type objectives have been used for 40 years in microscopy, especially for infrared or ultraviolet light. Fig. 3 shows the objective with two concentric spherical mirrors. The smaller convex mirror forms a strongly demagnified virtual intermediate image and the concave mirror with the central hole forms a weakly enlarged real image of the virtual image. The principal points of the objective coincide with the common center of curvature C. Since C lies outside the objective on the side where the specimen is placed, this mirror objective has a much larger working distance than a lens objective of similar focal length.

The aberrations of the concave and convex mirror have opposite signs and compensate each other. It was shown by Grey (1950) that in a concentric mounting there exists a

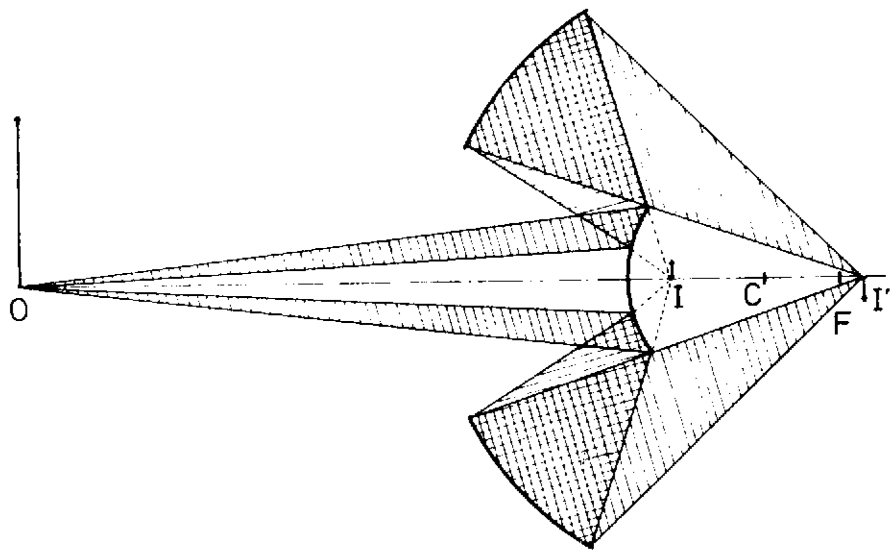

Fig. 3. Schwarzschild type objective with two spherical mirrors that have a common center of curvature C. The convex mirror forms a strongly demagnified virtual intermediate image I of the object O. The concave mirror forms a weakly enlarged image I' of I. F indicates the image side focal point.

ratio of radii of curvature where all third order aberrations vanish. For purely axial imaging as with a scanning microscope we could show that the resolution can be considerably improved by a slight deviation from concentricity. The central obstruction of about 20% of the area affects the resolution only near the diffraction limit (Sheppard, this conference; Staehr, 1980).

The objective of the prototype was obtained from Ealing and the mirrors were coated with seven layers of ReW/C optimized for λ = 200 Å. The objective has a numerical aperture of A = 0.27 and a focal length of f = 13.6 mm. The optical quality of the mirrors should meet the demands in the visible and near ultraviolet; the optical figure is specified as $\lambda/10$ (λ = 5500 Å).

The Scanning Principle

The scanning principle chosen for our microscope has some important advantages over a conventional setup.

(i) The radiation load of the specimen is reduced by some orders of magnitude. The multilayer coated Schwarzschild type objective acts as a coarse monochromator with low efficiency. In an imaging setup these losses would occur behind the fully irradiated specimen. In a scanning version the specimen is irradiated only by those photons which contribute to the image contrast.

(ii) The detector can be optimized for maximum efficiency, since it does not have to be position sensitive.

(iii) With on-axis imaging, only spherical aberrations are involved and the resolution of the Schwarzschild type objective is improved considerably.

(iv) Electronic signal processing and quantitative measurements are easily accomplished.

(v) The scale of magnification can simply be varied to get a quick survey of a large area or a detail with high accuracy.

On the other hand, a scanning system requires special properties of the light source. According to the laws of geometrical optics a reduction in source area is combined with a proportional increase in the divergency of the imaging light beam. This means that a light source of given area cannot arbitrarily be demagnified without a loss in the acceptance of the imaging system. The number of photons in the demagnified light spot therefore does not only depend on the intensity of the source, i.e. photons per second, but also on the brightness, i.e. intensity per source area and solid angle into which the light is emitted. In this respect, synchrotron radiation from a storage ring in the soft X-ray region is by at least one order of magnitude superior to all conventional light sources including characteristic lines of X-ray tubes (Kunz, 1974).

3. RESULTS AND DISCUSSION

Spectral Transmission of the Objective

The spectral transmission of the objective has been measured with the monochromator which is part of the microscope. The transmission curve, as displayed in Fig. 4, has a prominent peak at λ = 206 Å which is due to the multilayer coating. The relative width is 14% (FWHM). The rise in reflectivity for λ > 400 Å is not caused by interference but by a change in optical constants of the coating. This part of the spectrum can be suppressed by a carbon filter (see Fig. 1).

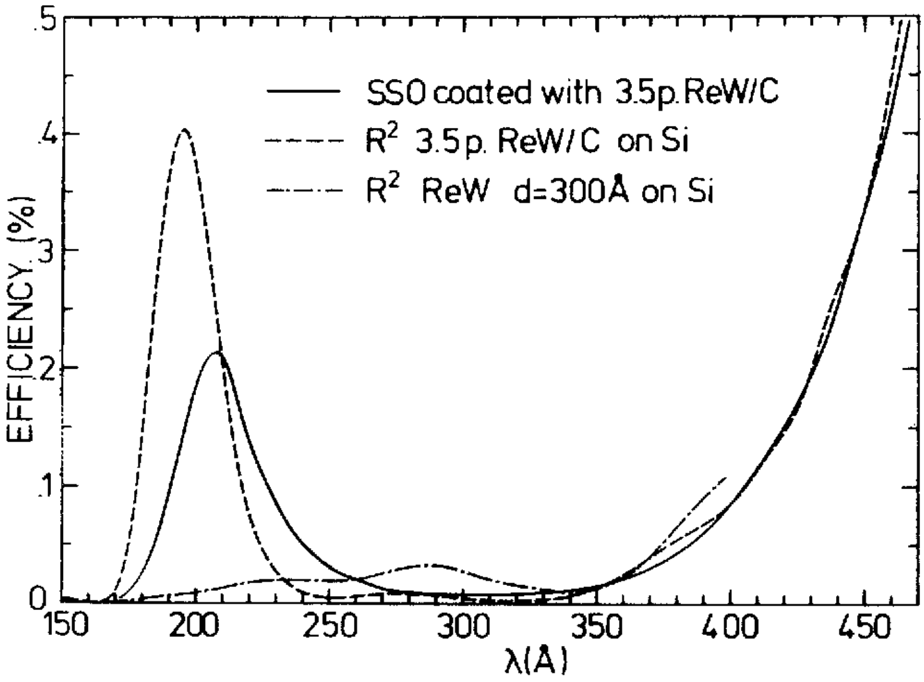

Fig. 4. Efficiency of the Schwarzschild type objective (SSO) coated with seven layers (= 3.5 periods) of Re W/C in comparison with the squared reflectivity of a simultaneously coated Si wafer and of a 300 Å thick film of ReW.

Simultaneously with the mirrors of the objective, we have coated a Silicon wafer. For comparison, its squared reflectivity is shown in Fig. 4 corresponding to the double reflection in the objective. The interference maximum is slightly shifted which can be explained partly by the fact that this measurement has not been carried out at normal incidence, but at an angle of $\alpha = 15^{o}$. The efficiency of the objective could be measured only in arbitrary units and has been fitted to the squared reflectivity of the same coating on the Si wafer in the long wavelength region. In this way, we obtained the absolute efficiency of 0.22% at the interference maximum of the multilayer coated objective. The different height of the reflectivity peaks is due to the uncertainty of the fit and to surface contamination of the objective mirrors which occurred during alignment in wet air.

In order to show how much is gained compared to a single film coating on the objective, also the squared reflectivity of a 300 Å thick film of ReW is shown in Fig. 4. If we assume that for a good image contrast not more than 20% spectral bandwidth is favorable, a gain factor of 14 is obtained. Moreover, a single film coating on the objective would require an extra monochromator introducing additional losses.

Resolution

In order to test the resolution of the microscope in one dimension we have scanned a razor blade edge through the focus. Fig. 5 shows the original line scan, made with a wavelength of $\lambda = 200$ Å. The image of the edge has a full width of about 2 μm. Scanning was done in steps of 400 Å. The counting rate was about 100 cts/sec on the clear side of the edge and for every picture element we counted about 30 seconds. Due to its usage by high energy physics the synchrotron was running with 1/100 of its optimum intensity; therefore, the total measuring time was 1 h 40 min.

The measured curve is the convolution of a step function, the ideal image of the razor blade edge as predicted by geometrical optics, and the point response, that is the intensity profile of the reduced image of the synchrotron light source. The point response which determines the resolution of the microscope can be calculated from the line scan (Haelbich, 1980) and is shown in Fig. 5. The obtained resolution can be approximated roughly by its halfwidth which is 1 μm (FWHM). The low intensity side maxima are due to statistical fluctuations of the measured curve, not to diffraction rings.

Fig. 5 shows that there is a background of about 20% of the maximum count rate at the dark side of the edge. To examine this more closely Fig. 6 presents the smoothed line scan over a wider range. Since the slope decreases very

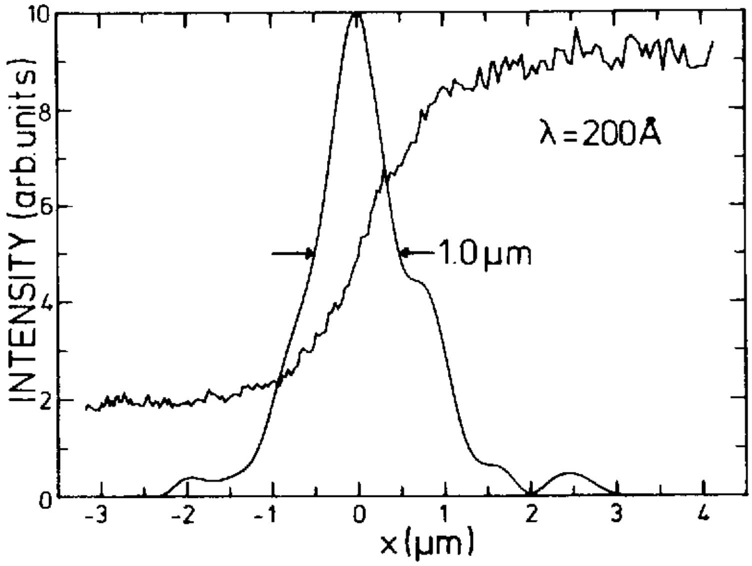

Fig. 5. Line scan of a razor blade edge at λ = 200 Å and deduced point response of the microscope.

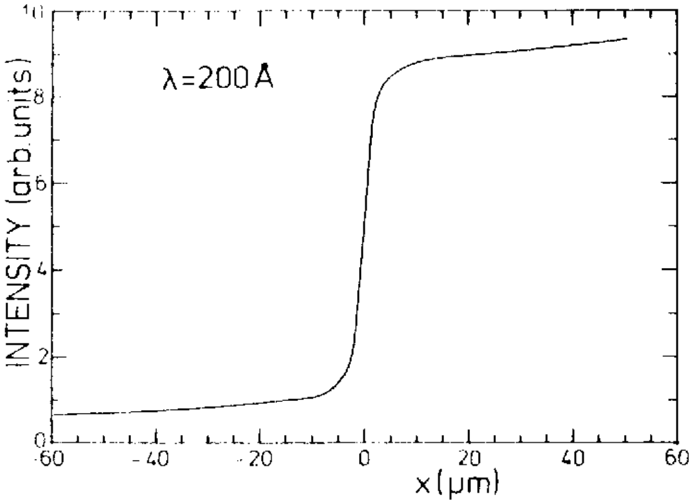

Fig. 6. Line scan of a razor blade edge at λ = 200 Å over an enlarged range which shows scattered background.

slowly, we conclude that the point response of Fig. 4 is positioned on a very flat background which is probably caused by surface roughness of the mirrors onto which the multilayer coating has been evaporated. This flat background deteriorates contrast and also resolution in the sense of a modulation transfer function.

As a second example for the imaging properties of the microscope Fig. 7 displays the line scan of a Fresnel zone plate with unsupported gold wires. The upper part of Fig.7 shows a region closer to the center of the zone plate where the period length is 7.2 μm. This measurement took one hour. At the left side there is a hole in the zone plate, the intensity there can be used to estimate the contrast. A detail from the outer part of the zone plate, where the period length is only 3.5 μm, is shown in the lower part of Fig. 7. The scanning speed has been reduced by a factor of 4 to improve statistics. The contrast is lower there and worse than expected from the line scan of the razor blade edge. This may be explained by vibrations of the unsupported wires or insufficient focussing.

According to the laws of geometrical optics, the Schwarzschild type objective images the illuminated pinhole as a disk with 0.7 μm diameter. The intensity rise at the rim of the disk should be very steep, since the resolution following the Rayleigh criterium is 450 Å. Reasons for deviations from this ideal image may be aberrations of the objective, bad optical figure of the mirrors or misalignment of the two mirrors.

To obtain the aberrations of the objective we carried out ray tracing calculations using a Monte Carlo procedure. With an optimum deviation from concentricity $\Delta d = 15.2$ μm the circle of least confusion produced by a point like object has a diameter of 600 Å which does not affect the resolution in our case. But the diameter of the circle of least confusion D_{LC} depends very sensitively on Δd as shown in Fig.8. Already, a misalignment of 80 μm would produce a circle of least confusion with $D_{LC} = 1$ μm. It is possible that the adjustment of the objective with visible light was not sufficiently sensitive.

The optical figure of the mirrors was quoted as $\lambda/10$ in the visible by the manufacturer. Staehr (1980) has tested similar objectives with the red laser line and could show that the diffraction patterns of the objectives agree very well with theory. From these results we expect that the optical figure of the mirrors allows a resolution of about 0.5 μm. Consequently, the optical figure may have broadened the resolution curve of our microscope by a small amount only.

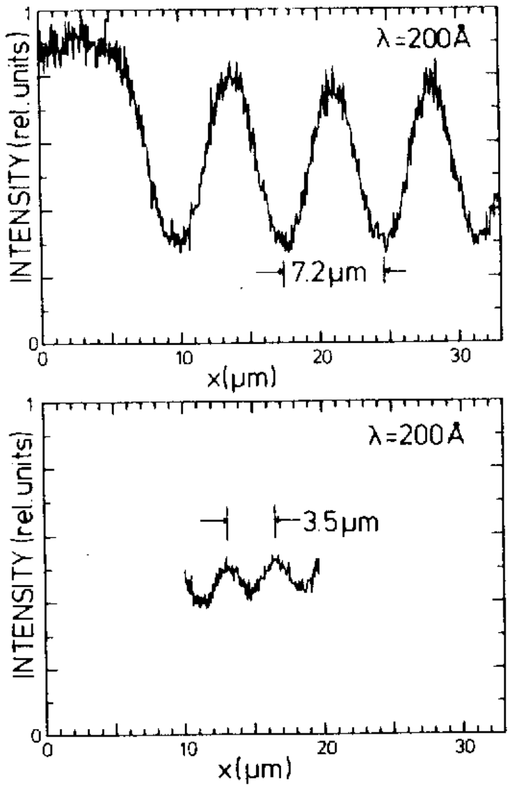

Fig. 7. Line scan of a Fresnel zone plate. At the top a detail near the center with 7.2 μm period length is shown, at the bottom a detail of the outer part with 3.5 μm period length.

The mirrors of the objective could not be aligned *in situ* but were adjusted with visible light beforehand. During the measurements with the microscope we made the observation that the resolution degraded with time. Realignment of the objective revealed a shift Δy_m of the convex mirror perpendicular to the optical axis. Fig. 9 shows the result of ray tracing calculations where we have simulated such a shift. On the left side, the pattern of intersection points of the calculated rays with the image plane is shown for an optimally adjusted objective; on the right side is demonstrated that already a shift of $\Delta y_m = 2$ μm is sufficient to produce a blur circle of 0.2 μm in diameter. This suggests that very small mechanical instabilities of the mirror mounting deteriorated the resolution and it explains why the intensity profile in Fig. 4 is not fully symmetric.

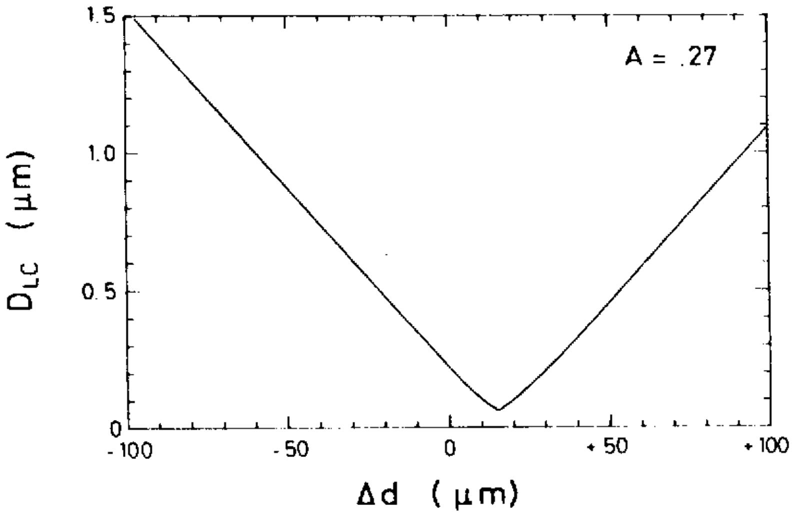

Fig. 8. Diameter of the circle of least confusion D_{LC} as function of the separation of the mirrors of the objective used in the experiments. Δd is the deviation from concentricity.

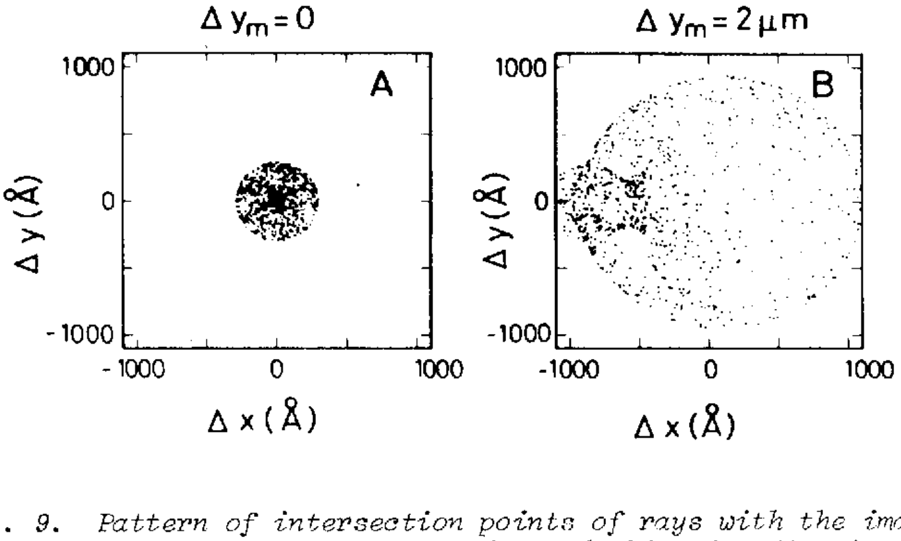

Fig. 9. Pattern of intersection points of rays with the image plane calculated for an optimal adjusted objective (left) and a deadjusted objective (right). The convex mirror has been shifted by Δy_m = 2 µm perpendicular to the optical axis.

4. FUTURE PROSPECTS

In order to make use of the advantages of soft X-ray microscopy, especially for biological applications, it is necessary to operate the microscope in the spectral region $\lambda < 100$ Å. Here the favorable contrast mechanisms compared to visible light and electron microscopy should be combined with a resolution which is considerably better than that of a light microscope. Based on our experience it shall be discussed whether our concept of ultrasoft X-ray microscopy with multilayer coated spherical mirrors for normal incidence can be further developed to meet these conditions: 300 Å resolution and a spectral range down to $\lambda = 45$ Å (carbon K-edge).

Resolution

The aim of our ray tracing calculations was to find the optimal parameters of a Schwarzschild type objective for on-axis imaging. Calculations were started with a concentric objective with a focal length of f = 20 mm and an imaging scale of 100 : 1 and then the deviation from concentricity was optimized as a function of the curvature radius R_1 of the convex mirror. The results are given in Fig. 10. The diameter of the circle of least confusion D_{LC} is shown for objectives of different numerical aperture A. The curves have sharp minima around $R_1 = 17$ mm (parameters see Table 1). For A = 0.2 it is possible to get a confusion circle with $D_{LC} = 2$Å and even for an objective with fourfold luminosity $D_{LC} = 82$ Å. The advantage of A = 0.2 is that $D_{LC} < 300$ Å independent of R_1.

As can be seen from Fig. 11, for the optimum configurations the optical path difference for rays with different inclination angle α to the optical axis is extremely small. For A = 0.2, the path difference ΔOPL in the annular aperture is smaller than 0.03 Å, for A = 0.3 smaller than 0.3 Å and for A = 0.4 about 8 Å.

This demonstrates that in principle it is possible to reduce the spherical aberrations of a Schwarzschild type objective with intermediate numerical aperture so strongly that diffraction limited imaging is possible on the optical axis.

The experiments with the prototype of our microscope have shown that the alignment of the mirrors is very difficult and may determine the achievable resolution. Table 2 lists how much deadjustment is tolerable so that D_{LC} does not exceed 300 Å. The alignment of the convex mirror perpendicular to the optical axis ist most difficult. Even for an

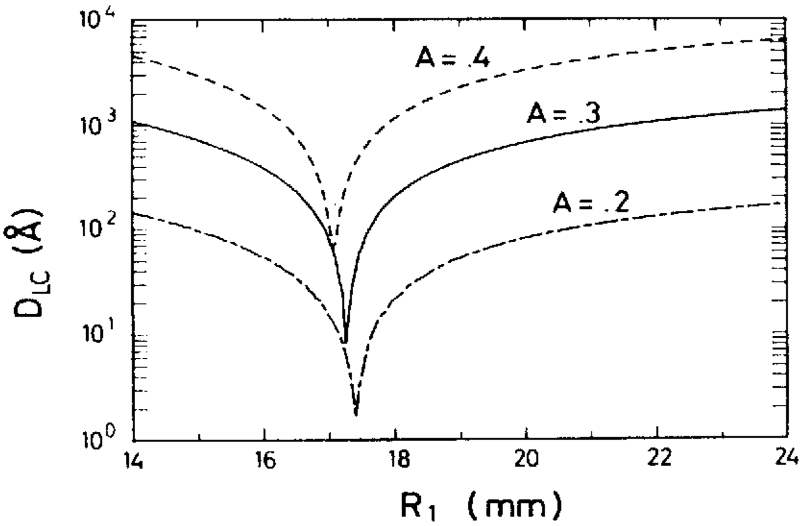

Fig. 10. Diameter of the circle of least confusion D_{LC} as function of the radius of curvature of the convex mirror R_1. The curves have been obtained by optimizing the deviation from concentricity for every R_1.

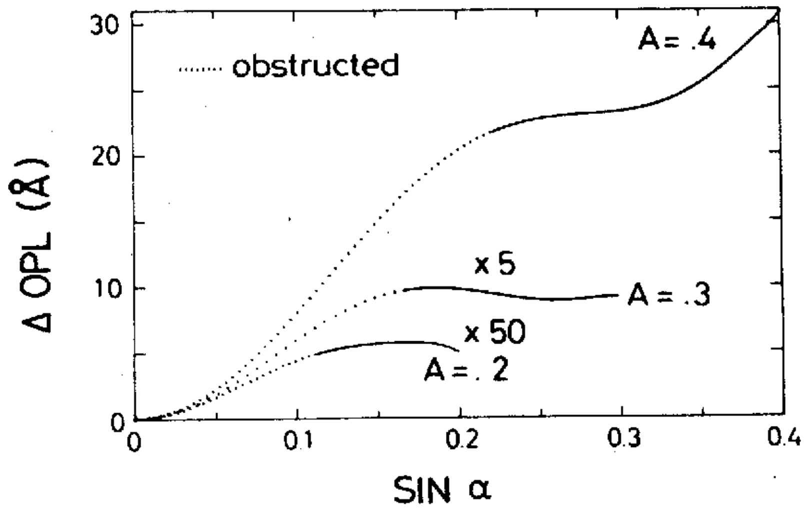

Fig. 11. Optical path difference ΔOPL for rays with different inclination angles α to the optical axis. For A = 0.2 the optical path difference has been scaled up by a factor of 50, for A = 0.3 by a factor of 5.

TABLE 1

Geometrical parameters of the optimal configurations of Schwarzschild type objectives according to Fig. 10

Numerical Aperture	A	0.2	0.3	0.4
Diameter of the circle of least confusion	D_{LC} (Å)	2	9	82
Radius of curvature of the convex mirror	R_1 (mm)	17.40	17.25	17.05
Radius of curvature of the concave mirror	R_2 (mm)	-30.80	-30.33	-29.72
Diameter of convex mirror	D_1 (mm)	6.9	10.3	13.6
Diameter of concave mirror	D_2 (mm)	18.3	26.8	34.5
Optimum deviation from concentricity	Δd_{opt}(mm)	1.0132	1.0171	1.0222
Focal length	f (mm)	17.37	17.31	17.22
Imaging scale	V	115	116	116
Linear central obstruction	ZA (%)	55	55	56

objective with A = 0.2 the convex mirror has to be centered better than 10 resolution elements. The least critical parameter is the off-axis position of the pinhole. To judge these results we have to take into account that the diameter of the circle of least confusion is a very strict criterion.

Misalignment is less critical for larger R_1, although the optimum resolution is slightly worse (Haelbich, 1980).

TABLE 2

Tolerable deadjustments of the optimal Schwarzschild type objectives (see Table 1) which expand the circle of least confusion to a diameter of D_{LC} = 300 Å

Numerical Aperture	A	0.2	0.3	0.4
Deviation from the optimum distance of the mirrors	$\lvert \Delta d - \Delta d_{opt} \rvert$ (μm)	2.40	0.70	0.28
Displacement of the convex mirror perpendicular to the optical axis	Δy_m (μm)	0.25	0.11	0.08
Off-axis position of the object	x_o (mm)	0.49	0.21	0.12

Optical Figure

The optical figure of the mirrors is of decisive importance. Each deviation δ of a part of the mirror from its ideal contour produces 2δ path difference. To get a resolution of 300 Å each mirror surface has to be accurate to approximately 30 Å which is about half of what can be done presently.

Multilayer Coatings

Multilayer coatings with C or B as spacer material can be used down to their K-edges at λ = 45 Å or λ = 67 Å, respectively. Since the absorption of the highly and weakly absorbing component is decreasing with wavelength, more layers have to be added to get good reflectivity at shorter wavelengths, but the highest reflectivity attainable with an infinite number of layers is also increasing to theoretically 30 - 50% at normal incidence in the region λ < 100 Å. For microscopy purposes about 30 - 50 periods are necessary to get maximal integrated reflectivity. Using optical constants of Hagemann *et al.* (1975), it has been calculated (Haelbich, 1980) that an objective coated with 30 periods of Au/C would have an efficiency of more than 1 percent averaged over a spectral bandwidth of 3% for λ = 50 Å.

As already mentioned, thickness control with an oscillating quartz is not applicable for more than seven layers. Spiller *et al.* (1980a) have developed a new procedure which allows evaporation of a large number of layers all contributing constructively to the reflected wave. The basic idea is

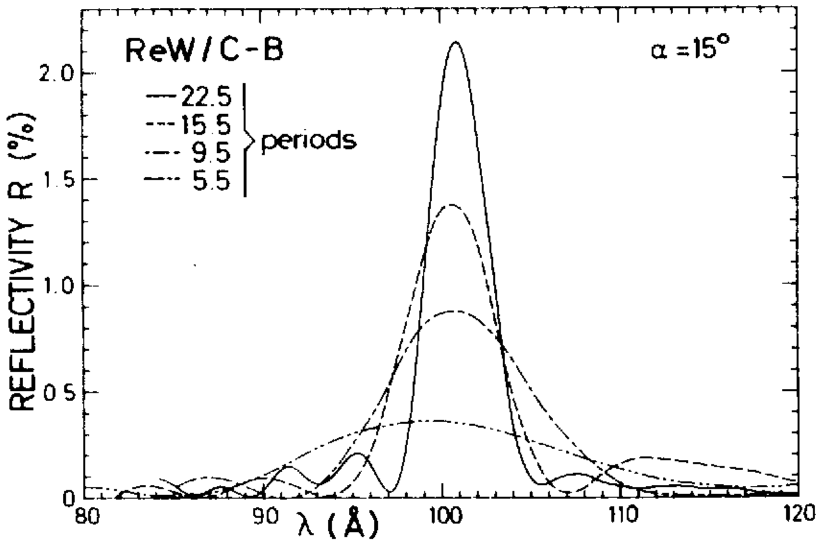

Fig. 12. Measured reflectivity of 11, 19, 31 and 45 layers of ReW/C-B at an angle of incidence α = 15°. The thickness of the layers was monitored by reflection measurements at λ = 44.8 Å and α = 63° during deposition. The coatings with less than 45 layers were prepared by partly shadowing the substrate during deposition.

to measure the reflectivity at oblique incidence during deposition with soft X-rays. The reflectivity is oscillating as function of film thickness and the extrema indicate where to end one layer and start with the other material. Fig. 12 shows one of the first results with this technique: 45 layers (= 22.5 periods) of ReW/C-B optimized for λ = 100Å. Part of the spacer layers consisted of B instead of C, because this facilitates thickness control. The samples with less than 45 layers were prepared by partly shadowing the substrate. The increase of reflectivity with the number of layers demonstrates that it is possible to evaporate 45 layers without detrimental thickness error. Compared to a single thick film of ReW, the peak reflectivity of 45 layers is larger by a factor of 120. Further results with the new preparation technique are given by Spiller *et al.* (1980b).

Surface Roughness

If the root mean square surface roughness σ is larger than 1/20 of the wavelength λ, diffuse scattering cannot be neglected compared to specular reflection at normal incidence. Therefore, surface roughness may very well limit the application of multilayer coatings for short wavelengths. For an eleven layer coating deposited on a chemically polished single crystal of Silicon we have derived an effective surface roughness of $\sigma = 3$ Å (Haelbich et al., 1979) which may be essentially the surface roughness of the substrate. Following scalar theories (Bennet and Porteus, 1961) even this extremely small surface roughness produces as much diffusely scattered light as specular reflected at $\lambda = 50$ Å; this means the usable efficiency of the objective is reduced by a factor of 4. The best finish of spherical surfaces is in the order of 8 Å limiting the spectral range to $\lambda > 80$ Å. But Spiller *et al.* (1980a) have observed that multilayer coatings of ReW/C do not only add no surface roughness to that of the substrate but even appear to have a smoothing effect that would allow to use spherical mirrors also for shorter wavelengths.

Efficiency of the Microscope

To estimate the counting rate of an improved microscope we proceed with the storage ring DORIS as synchrotron radiation source which has a brightness of $5 \cdot 10^{20}$ photons per sec/cm^2/sterad/eV at a photon energy of 250 eV (Kunz, 1974). A microscope with a numerical aperture of 0.3, a resolution of 300 Å and a bandwidth of 3% can accept $6 \cdot 10^9$ photons/sec. The reflections including scattering will cost 3 – 4 orders of magnitude. The resultant counting rate of 10^6 photons/sec allows a scanning speed of about 3000 picture elements/sec which gives a scanning time of a little more than a minute for an image of 500 x 500 picture elements.

Comparison with other Methods

Our way of using multilayer coated spherical mirrors at normal incidence is competing with the use of Fresnel zone plates (see Schmahl, this conference) and mirrors for grazing incidence (Silk, 1980). Both methods have the advantage that the wavelength can be varied over a quite wide range with the same imaging element, while the special multilayer coating fixes the wavelength. Additionally with multilayer coatings and normal incidence reflections difficulties are increasing with decreasing wavelength. The theoretically obtainable resolution of all these imaging elements is about the same. While Schmahl *et al.* (1980) have already reached 700 Å resolution with a zone plate microscope, grazing incidence objectives with necessarily two aspheric mirrors have not gained a resolution of much better than 1 μm (Silk, 1980), although much effort has been spent thereon. Concerning efficiency, the Schwarzschild type objective may be favored at least to a zone plate whose efficiency decreases with increasing resolution. For some applications also the long working distance of the Schwarzschild type objective is of some advantage.

5. SUMMARY

I have reported a new way of ultrasoft X-ray microscopy whose most important characteristic is the use of multilayer coated spherical mirrors at normal incidence.

The scanning principle is essential for this microscope, since it reduces radiation damage of the specimen by orders of magnitude and makes use of the improved resolution on the optical axis. On the other hand, it requires the brightness of a synchrotron radiation source.

We have constructed a prototype of the microscope and obtained a resolution of 1 - 2 μm at a photon energy of 60eV during the first tests; the resolution has been limited mainly by the difficult adjustment of the objective under the low intensity conditions of a synchrotron operating at 1/100 of its optimum intensity.

The future prospects of the microscope have been discussed. The most important result is that we were able to demonstrate by ray tracing calculations that aberrations can be minimized so far that diffraction limited imaging even in the soft X-ray region is possible. The deposition of multilayer coatings has reached a stage where the spectral region $\lambda < 100$ Å is accessible. Future work has to prove that problems arising from optical figure and surface roughness can be coped with.

ACKNOWLEDGMENT

The author thanks W. Staehr for testing part of the microscope in the visible and C. Kunz and E. Spiller for several useful discussions.

REFERENCES

Bennet, H.E. and Porteus, J.O. (1961). Relation between Surface Roughness and Specular Reflectance at Normal Incidence, *J. Opt. Soc. Am.* 51, 123-129.

Grey, D.S. (1950). A New Series of Microscope Objectives. III. Ultraviolet Objectives of Intermediate Numerical Aperture, *J. Opt. Soc. Am.* 40, 283-290.

Gudat, W. (1978). Soft X-Ray Microscopy and Lithography with Synchrotron Radiation, *Nucl. Instr. Methods* 152, 279.

Haelbich, R.-P. and Kunz, C. (1976). Multilayer Interference Mirrors for the XUV Range around 100 eV Photon Energy, *Opt. Commun.* 17, 287-292.

Haelbich, R.-P., Segmüller, A. and Spiller, E. (1979). Smooth Multilayer Films Suitable for X-Ray Mirrors, *Appl. Phys. Lett.* 34, 184-186.

Haelbich, R.-P. (1980). "Untersuchung der Eigenschaften von Mehrschichtinterferenzspiegeln aus absorbierenden Materialien und ihre Verwendung in einem Rastermikroskop für weiche Röntgenstrahlung." Thesis, Universität Hamburg. *Internal Report DESY F41 HASYLAB* 80/3.

Hagemann, H.J., Gudat, W. and Kunz, C. (1975). Optical Constants from the Far Infrared to the X-Ray Region: Mg, Al, Cu, Ag, Au, Bi, C and Al_2O_3, *J. Opt. Soc. Am.* 65, 742-744 and *Internal Report DESY* SR-74/7.

Kunz, C. (1974). Perspectives of Synchrotron Radiation - Report on a Panel Discussion. *In* "Vacuum Ultraviolet Radiation Physics" (Ed. E.E.Koch, R. Haensel and C. Kunz) p. 753. Pergamon-Vieweg, Braunschweig.

Schmahl, G., Rudolph, D., Niemann, B. and Christ, O. (1980). X-Ray Microscopy of Biological Specimen with a Zone Plate Microscope, *Ann. N.Y. Acad. Sci.* 342, 368-386.

Schwarzschild, K. (1905). "Untersuchung zur geometrischen Optik II, Theorie der Spiegelteleskope" Abh. Königl. Ges. Wiss., Göttingen.

Silk, J.K. (1980). A Grazing Incidence Microscope for X-Ray Imaging Applications. *Ann. N.Y. Acad. Sci.* 342, 116-129.

Spiller, E. (1972). Low-Loss Reflection Coatings Using Absorbing Materials, *Appl. Phys. Lett.* 20, 365-367.

Spiller, E., Segmüller, A. and Haelbich, R.-P. (1980a). The Fabrication of Multilayer X-Ray Mirrors, *Ann.N.Y. Acad. Sci.* 342, 188-200.

Spiller, E., Segmüller, A., Rife, J. and Haelbich, R.-P. (1980b). Controlled Fabrication of Multilayer Soft X-Ray Mirrors. *Appl. Phys. Lett.*, in press.

Staehr, W. (1980). "Untersuchung der optischen und mechanischen Eigenschaften eines Rastermikroskops mit Spiegelobjektiv im Hinblick auf die Verwendbarkeit im weichen Röntgengebiet" Diploma Thesis, University of Hamburg.